Brief report

NoxO1 Determines Level of ROS Formation by the Nox1 Centered NADPH Oxidase

D. Maureen Hebchen[1], Manuela Spaeth[1], Niklas Müller[1] and Katrin Schröder[1,2*]

[1] Institute for Cardiovascular Physiology, Goethe University Frankfurt, Germany
[2] German Center of Cardiovascular Research (DZHK), Partner site RheinMain, Frankfurt, Germany
* Correspondence: author: E-Mail: Schroeder@vrc.uni-frankfurt.de

Abstract: Activity of the Nox1 centered NADPH oxidase complex depends on the activator NoxA1 and the organizer NoxO1. NoxO1 itself is not involved in electron transfer for superoxide formation. Instead, by creating proximity of all components in the right place NoxO1 enables a constitutive formation of reactive oxygen species by that complex. All subunits should form the complex in a 1:1:1 ratio. When analyzing different cell lines in this study, we found an unequal expression of the component on mRNA level with an excess of NoxO1. Even with plasmid-based overexpression of individual components of Nox1 centered NADPH oxidase complex results in different expression of their mRNA, with NoxO1 mRNA being best expressed. Despite an unchanged high level of NoxO1 mRNA over a wide range of transfected plasmid, protein expression is increased with accelerating plasmid concentrations. We thought to analyze the ability of NoxO1 to induce ROS formation, when present in different ratio to Nox1 and NoxA1. To this end, we used Hek293 cells with constitutive expression of Nox1 and NoxA1 transfected with increasing concentrations of NoxO1. Our results suggest that ROS formation by the Nox1 centered NADPH oxidase strongly depends on the level of NoxO1 and a surplus of NoxO1 further increases the activity of the complex.

Keywords: NoxO1; Nox1; NoxA1; reactive oxygen species

1. Introduction

The family of NADPH oxidases represents a source of reactive oxygen species (ROS), which consists of seven members, Nox1-Nox5 and Duox1 and Duox2. Out of those, Nox1-3 are able to form complexes with cytosolic subunits, which enables activity of the mentioned NADPH oxidase complexes and subsequent ROS formation. Cytosolic subunits display activating (p67phox and NoxA1) or organizing (p47phox and NoxO1) features [1]. Numerous homologue-specific mechanisms control assembly of the NADPH oxidase complexes involving, free fatty acids, intracellular trafficking, and posttranslational modifications such as phosphorylation, acetylation, or sumoylation [2]. For activation of Nox1 mediated ROS formation, the cytosolic subunits NoxA1 and NoxO1 have to complex with the membrane bound subunits Nox1 and p22phox. Binding of the subunits is facilitated via several sites in each protein. NoxO1 has a PX (phox homology) domain for translocation to the plasma membrane, a proline rich region for interaction with NoxA1 and 2 SH3 (Src homology) domains for interaction with p22phox [3]. The stoichiometry of all subunits in the active Nox1 complex is anticipated to be 1:1:1. This is especially likely, when taking into account that the one prolin rich region of NoxO1 can only bind the one SH3 domain in NoxA1.

NoxO1 is of special interest as due to a missing inhibitory loop it mediates constitutive superoxide formation by the Nox1 centered NADPH oxidase [4]. This constitutive ROS formation can alter a cells phenotype [5] and Nox1/NoxA1/NoxO1 mediated ROS formation may have detrimental effects. In a recent publication a newly discovered biflavonoid exhibits cytotoxic effects to MCF7 breast cancer cells, among others via downregulation of NoxO1 mRNA expression [6]. That implies that NoxO1 has pro-survival effects

 doi:10.20944/preprints202303.0002.v1

in breast cancer. In contrast, others describe detrimental roles of NoxO1 in cancer. Ubiquitination of NoxO1 by the deubiqitinase cylindromatosis (CYLD) reduces its protein half-life as well as NoxO1 mediated ROS formation in PC3 cells [7]. Knockout of CYLD in PC-3 cells promoted proliferation, migration, colony formation and invasion in vitro and injection of CYLD-depleted cells into xenografted mice forced tumor development. This result is consistent with a study performed in our lab, where we provide evidence that loss of NoxO1 in mice results in less differentiation of enterocytes and spurs DSS/AOM induced colitis and cancer formation [8]. In contrast, inflammatory bowl disease is associated with TNFα/NFκB induced expression of NoxO1 and increased Nox1 derived ROS formation [9,10]. In stomach, NoxO1 potentially has pro-tumorigenic functions. In inflammatory settings TNFα induces NoxO1 expression and subsequent Nox1 dependent ROS formation, which results in enhanced proliferation of stomach epithelial cells and eventually cancer formation [11]. In line with that a potential role of Nox1 centered NADPH oxidase in gastric inflammation was proposed [12]. The potential role of Nox1 and its cytosolic subunits in cancer undelines the need for a better understanding of this NADPH oxidase.

Many studies focus on expression of Nox1, NoxA1 and NoxO1 or just on Nox1, when analyzing the effects of this NADPH oxidase. With this study, we aim to contribute knowledge of the composition of the NADPH oxidase needed for proper activity. We investigate the role of NoxO1 for Nox1 mediated ROS formation.

2. Materials and Methods

If not stated otherwise, human genes and proteins are addressed.

2.1. Cell lines and cell culture

Human cell lines (HEK293, Caco-2, MDA-MB231; MCF7) were purchased from ATTC (Manassas, USA). All cells were cultivated in Minimal Essential Medium (MEM,#11095080, Gibco) with 1 mM Sodium pyruvate (#M7145, sigma), 0.1 mM Non-essential Amino acids (#S8636, sigma), 0.5 % Penicillin-Streptomycin (#15140-122, 10000 U/ml,) and 8-20% fetal calve serum (#f7524, sigma). For MDA-MB231 and MCF7 cells, 0.01 mg/ml human insulin (#I9278, sigma) was supplemented. Cells were cultured under 5 % carbon dioxide atmosphere at 37°C. Cells were passaged weekly and supplied with fresh culture media every 3-4 days.

2.2. mRNA espression in murine tissue and in cell lines

For determination of Nox mRNA expression in murine tissue, adult male or female C57Bl6 mice were terminally anaesthetized with isoflurane (Piramal) and subjected to cervical dislocation. Biopsies were taken from colon, lung, mammary gland, testes and pancreas. Tissue samples were snap-frozen in liquid nitrogen and stored at -80°C. Before RNA isolation, tissue was lysed in the Tissue Lyser (Qiagen).

Whole-cell RNA from tissue and cell lines was isolated with the Bio&Sell RNA Mini Kit according to the manufactorer's instructions. Reverse transcription was performed by rt-SuperScript™ III (#18080093, Invitrogen) and random primers (#C1181, Promega). cDNA was amplified in an qRT-PCR in an Aria MX thermocycler (Agilent) using ITaq UNIVERSYBR® Green SMX 5000 (#1725125, BioRad) referring to ROX dye as reference. qRT-PCR samples were performed in technical duplicates. Target gene expression was normalized to GAPDH using Δct or relative expression using the ΔΔct method, respectively. Primers used in qRT-PCR are listed in table 1.

 doi:10.20944/preprints202303.0002.v1

Table 1. Primers for qRT-PCR.

gene	forward (5′-3′)	reverse (5′-3′)
GAPDH	TGCACCACCAACTGCTTAGC	GGCATGGACTGTGGTCATGAG
mNoxo1	TGGAGGAGGTAGCAACGTGC	AGAGCGACTGCCCTCGTAGG
Nox1	TCTTATGTGGCCCTCGGACT	CCAGACTGGAATATCGGTGACA
Noxa1	TGGGAGGTGCTACACAATGTG	TTGGACATGGCCTCCCTTAG
Noxo1	GAGATCTGACCGCGTTCTCC	CAGCAGCCTCCGAGAATAGG
p47phox	ACGAGTTCCATAAAATGCTGAAGG	GAGATCTTCACGGGCAGTCC
p67phox	ACCTTGAACCAGTTGAGTTGCG	GTCGGACTGCGGAGAGCTT

2.3. Overexpression systems

For transient overexpression, cells were seeded on 6-well plates to reach 70-80% confluence and transfected with plasmids coding for Nox1, NoxA1 or NoxO1. All vectors were designed on a pCMV6-Entry backbone with C-terminal myc- and flag-tag for easier detection. Transfection was carried out with 1 µg/ml polyethyleneimine (PEI, #408727, sigma) or with the Lipofectamine3000® Kit (#L3000001, Invitrogen) for 4-6 h at 37 °C in MEM without supplements. After exchange of MEM to growth media (see section cell lines), overexpression was allowed for 1 day before performing experiments.

Constitutive overexpression of NoxO1 or NoxA1 and Nox1 was generated by lentiviral transduction followed by selection with 400 µg/ml Hygromycin (#ALX-380-309-G001, Enzo) or 2 µg/ml Puromycin (#0240.4, Carl Roth). Lentiviral vectors were based on a pLV-EF1a-IRES-Hygro (#85134, addgene) or pHAGE2-EF1aFull-hOct4-F2A-hKlf4-IRES-hSox2-P2A-hcMyc-W-loxP (kindly provided by Dr. Gustavo Mostoslavsky) backbone. Lentiviral particles were produced in Lenti-X™ 293T cells (purchased from Takara) by transfection with 1 µg/ml PEI together with the packaging plasmids psPAX2 / pmD2.G (#12260, #12259, Addgene) and the Nox-encoding plasmid. After 1-2 days, lentiviral particles were harvested from the supernatant and tested with Lenti-X™ GoStix™ Plus (#631280, Takara). Host cells were infected with 1 ml supernatant and 8 µg/mL Polybrene (#TR-1003-G, Merck) for 1 day. Selection was started after 1-2 days. As control, cells were transducted with an empty vector construct. Functionality of the overexpressed protein was verified by the ability to produce reactive oxygen species (ROS) after co-transfection of the missing Nox subunits (see section ROS measurement). All plasmids were verified by Sanger sequencing at Microsynth Seqlab GmbH (Göttingen, Germany).

Table 2. shows an overview of plasmid constructs used for this study.

protein expressed		backbone	tag for detection
Nox1	transient	pCMV.6-entry	c-myc, Flag-DDK
NoxA1			
NoxO1			
eGFP		pEGFP-C1	GFP
(empty vector)		pLV-EF1a-IRES-Hygro	
NoxO1			

 doi:10.20944/preprints202303.0002.v1

	constitutive		-
Nox1+NoxA1		EF1aFull-hOct4-F2A-hKlf4-IRES-hSox2-P2A-hcMyc-W-loxP	

Table 2: plasmids used

2.4. ROS measurement with chemiluminescence

For ROS measurements, cells were seeded on 6-well-plates to reach 70-80% confluence and transfected with plasmids coding for Nox1, NoxA1 or NoxO1 (see section overexpression systems). As control, cells were transfected with a plasmid coding for eGFP (pEGFP-C1, #2487, addgene). Living cells were scraped from the dish and resuspended in HEPES-Tyrode buffer (137 mM NaCl #31434-5KG-R, 2.7 mM KCl # P9333, 0.5 mM MgCl # M8266, 1.8 mM CaCl2 # C7902, 5 mM D-Glucose #16301, 0.36 mM NaH2PO4*H2O # 106346, 10 mM HEPES # H-3375, all from sigma) with 200 µM L-012 (8-Amino-5-chloro-2,3-dihydro-7-phenyl-pyrido[3,4-d]pyridazine sodium salt, #120-04891, WAKO Chemicals). ROS production was assessed by L-012 chemiluminescence at 37°C in a 6-channel luminometer. For quenching of superoxide, 20 U superoxide dismutase (SOD, #S7571, sigma) was added at the end of each measurement.

2.5. Immunofluorescence and confocal microscopy

Cells were seeded on 8-well µ-slides (ibidi) and cultivated until 70-80% confluence. In order to determine NoxO1 expression in transient overexpression, cells were transfected with varying amounts of plasmid (see section overexpression systems). After 1 day of overexpression, cells were fixed with Roti® Histofix (#P087.1, Carl Roth) for 20 min, washed with Dubecco's Phosphate-buffered saline (DBPS, #14040133, Gibco) and 2% L-glycine (#A1377,5000 AppliChem) to remove residual paraformaldehyde. Cells were permeabilized with 0.05 % Triton-X 100 (#3051.3, Carl Roth) for 10 min. Unspecific binding sites were blocked with 3 % bovine serum albumin (BSA, #A8412, sigma) for 1h. Myc-tagged NoxO1 was detected by a primary goat-anti myc antibody (#A190-104A, Bethyl/Biomol), diluted 1:300, overnight at 4°C. The next day, unbound antibody was removed with 0.03 % Tween20® (#12377433, fisher) .For 1-2 h samples were incubated at room temperature with AF488-conjugated donkey anti-goat secondary antibody (#A11055, Invitrogen), diluted 1:500. Nuclei were stained with 0.1 µg/ml DAPI (4',6-Diamidino-2-phenylindole dihydrochloride, #D9542, sigma) for 15 min at room temperature. Finally, slides were washed with 0.03 % Tween20® and DPBS, respectively. Slides were stored in the dark until detection with a confocal laser scanning microscope (LSM800, Zeiss). Images were processed with Zen blue (3.3 edition, Zeiss) and ImageJ (1.53q).

2.6. NoxO1 protein expression

HEK293 cells transiently overexpressing NoxO1 were lysed (250 mM Tris*HCl pH7.4 #AE15.3 Carl Roth, 750 mM NaCl #S/3160/65 fisher, 50mM Na4PPi # 106391 Merck, 100mM NaF #201154 sigma, 10% Triton-X #3051.3 Carl Roth, 2 mM Orthovanadate #A2196 AppliChem, 10 mM Okadaic Acid #ALX-350-011 Enzo, 200 µM PMSF #6367.1 Carl Roth, 20 µM cOmplete ##4693116001, Merck). After centrifugation (10 min, 4 °C, 13000 rpm), nuclear fraction was discarded.Total protein amount in the cytosolic fraction was quantified by photometric Bradford assay with Roti-Quant® (#K015.1, Carl Roth). Samples were boiled for 10 min at 95 °C in Laemmli buffer (25.5% glycerol #G7893 sigma, 6% SDS # L-4390 sigma, 188 mM Tris*HCl pH 6.8 #AE15.3 Carl Roth, 60 mM DTT # A1101 AppliChem, 0.04% bromphenolblue #A3640,0005 AppliChem). Proteins were separated by Sodium-Dodecylsulfate-Polyacrylamide-Gel-Electrophoresis (SDS-PAGE) on 10% acrylamide gels followed by Western Blot. NoxO1 was detected through flag- or myc-tag (#A190-104A Bethyl, #F7425 sigma) and normalized to ERK (#4696, Cell Signaling) expression.

 doi:10.20944/preprints202303.0002.v1

2.7. Statistical analysis

Data are presented as mean and standard error of the mean (SEM). All experiments were at least conducted in three independent biological samples with duplicates. Each sample is defined by "n". Calculations and statistical analysis were performed with Prism 9 (Graph Pad) and Excel2016.

3. Results

According to ProteomicDB [13] NoxO1 protein in human and mouse is mainly expressed in stomach, colon and rectum, while according to GTExPortal [14] NoxO1 mRNA in human is mainly expressed in testis, brain and small intestine. Our own analysis of murine tissue revealed a high expression of NoxO1 mRNA in colon, breast and pancreas (**Supplemental figure 1**). Given the potential role of NoxO1 in cancer, further analysis concentrated on colon and breast cancer cell lines (CaCo2, MCF7 and MDA-MB231) as well as Hek293 cells as models. When analyzing for expression of the large membrane bound subunits of each NADPH oxidase (**Figure 1**), as expected found Nox1 mRNA to be highest expressed in CaCo2 cells. Nox2 mRNA expression was highest in Hek293, followed by MDA-MB231 cells. Nox3 is largely exclusive for the inner ear and accordingly was if at all, Nox3 mRNA is expressed at very low levels throughout all analyzed cell lines. Nox4 mRNA expression was quite low as well and surprisingly CaCo2 and MCF7 cells show highest values. Nox5 mRNA was highest expressed in MCF7 and Duox1 and 2 were highest in MDA-MB231 cells.

Preprints (www.preprints.org) | NOT PEER-REVIEWED | Posted: 1 March 2023 doi:10.20944/preprints202303.0002.v1

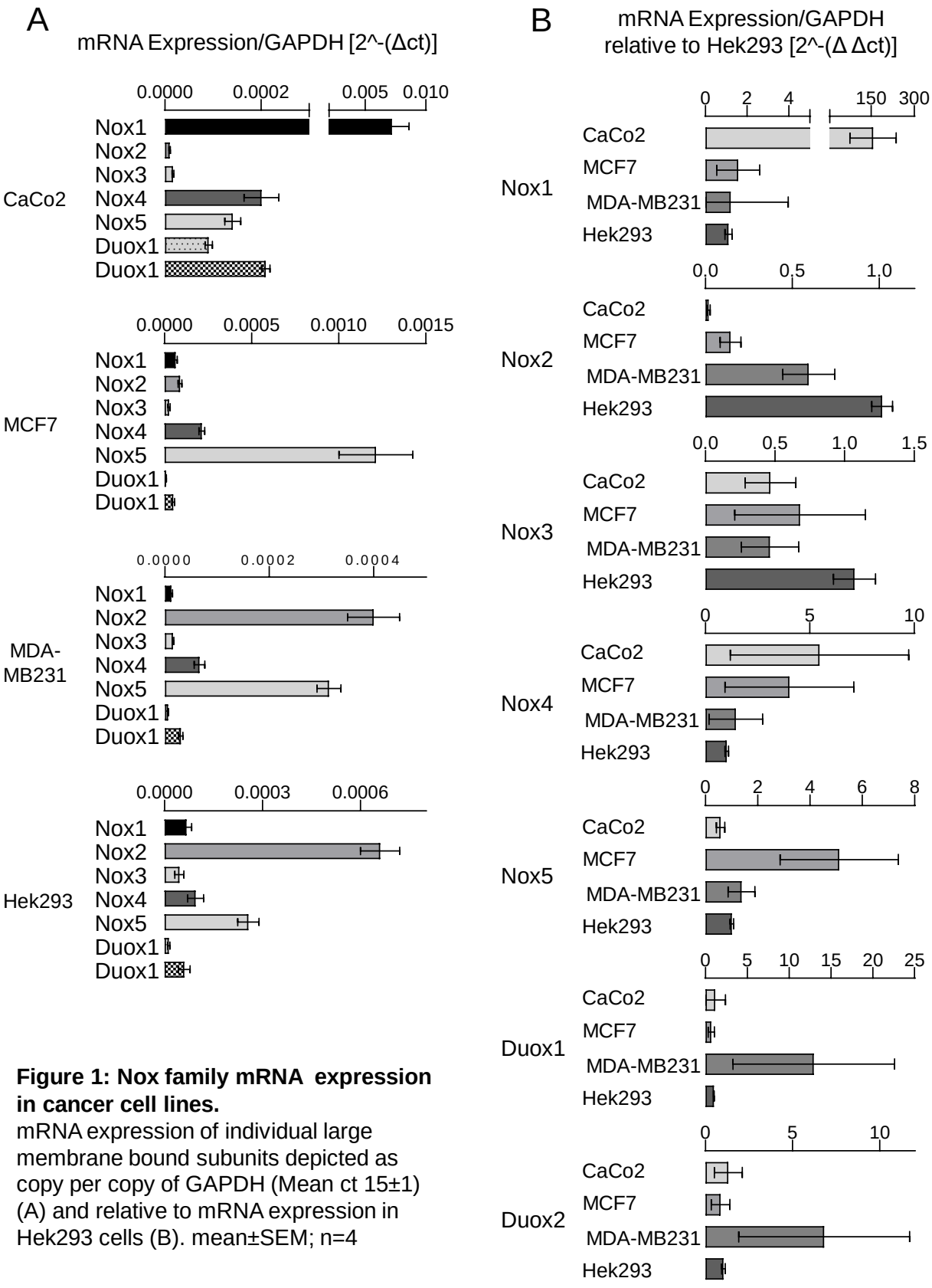

Figure 1: Nox family mRNA expression in cancer cell lines.
mRNA expression of individual large membrane bound subunits depicted as copy per copy of GAPDH (Mean ct 15±1) (A) and relative to mRNA expression in Hek293 cells (B). mean±SEM; n=4

 doi:10.20944/preprints202303.0002.v1

Diving deeper into more detailed analysis of the Nox1 centered NADPH oxidases in the selected cell lines revealed the same level of Nox1 and NoxO1 in CaCo2 and in all others a surplus of NoxO1 mRNA (**Figure 2**). When overexpressing all three components of the Nox1 centered NADPH oxidase, expression level strongly depend on transfection efficacy. Besides that, even in cells easily to transfect, expression of the components was not equal within and between the cell lines, with major intra cell-line inequality in Hek293 cells. The question, if either of the components alters the expression of the others remains unanswered here. Our data implies that in Hek293, overexpression of one subunit does not reduce basal mRNA level of the others. It rather induces expression of other components of the complex (**Supplemental figure 2**). This phenomenon however, needs much more detailed analyses in cells expressing higher endogenous expression of Nox1 centered NADPH oxidases in order to avoid false data due to very low expression levels of the components. When analyzing overexpression of the single subunits in more detail, we found a stepwise increase over a certain range of plasmid amount transfected per cm^2 (**Figure 3**). Interestingly, mRNA expression reaches a plateau for all three components at different plasmid concentrations transfected: Nox1 0.1, NoxA1 0.05 and NoxO1 0.015 $\mu g/cm^2$. Even the plateau height differs among the subunits. Nox1 and NoxA1 reach a similar level of expression, while NoxO1 expression massively exceeds Nox1 and NoxA1. In case of NoxO1, reaching a plateau is potentially not evident on protein level (**Figure 4**). In immunofluorescence it appears that NoxO1, if expressed at concentrations below 0.1 $\mu g/cm^2$, stacks in the perinuclear endoplasmic reticulum. If transfected with 0.1 µg plasmid/cm^2, NoxO1 mainly appears at the plasma membrane and with increasing plasmid load the whole cell is flooded with NoxO1 (**Figure 4A&B**). Interestingly, transfection efficacy is not increased with more plasmid. The percentage of cells hit by the transfection reagents remains relatively constant. Different from immunofluorescence based analysis detection, NoxO1 abundance in Western blot analysis reveals a strong expression of the protein even when cells were transfected with as few as 0.01 µg plasmid /cm^2. With increasing concentration of plasmid, NoxO1 expression increases accordingly up to 0.1 $\mu g/cm^2$. Due to a lack of proper antibodies for NoxO1, we were not able, to detect NoxO1 itself, but had to tag the protein. From the above experiments, we concluded that little NoxO1 plasmid amount results in a proper expression of the protein. The next step was to discover, if the protein produced is functional. As mediation of ROS formation by the Nox1 centered NADPH oxidase is the only known function of NoxO1, we measured ROS formation. When overexpressing all components of the Nox1 centered NADPH oxidase with plasmid concentration of 0.01 $\mu g/cm^2$ no ROS formation greater than those of GFP transfected cells was observed, while from 0.05 µg plasmid/cm^2 the ROS formation detected was not further increased by higher plasmid concentration (**Supplemental figure 3B**). The same hold true for CaCo2 cells, while MCF7 and MDA-MB231 cells do not generate ROS, when transfected with the components of Nox1 centered NADPH oxidase (**Supplemental figure 4**), potentially because transfection efficacy is low as seen in figure 2. Importantly, we found no basal ROS formation in any of the cells analyzed. We generated Hek293 cells with constitutive NoxO1 expression (Hek293-cNoxO1), which express 500 time more NoxO1 mRNA that native Hek293 cells (**Supplemental figure 3A**). In those cells, we found similar results as with native Hek293 overexpressing all subunits: no ROS formation at 0.01 and plateau at 0.05µg plasmid/cm^2 (**Supplemental figure 3C**). We conclude, the effect seen in Figure 2 that NoxA1 mRNA expression in triple transfected cells is much less, than that of Nox1 and NoxO1 persists and results in too little NoxA1 protein. So, we generated Hek293 cells with constitutive Nox1 and NoxA1 expression (Hek293-cNox1/NoxA1), which express 1200 times more Nox1 and 500 time more NoxA1 mRNA than native Hek293 cells (**Supplemental figure 3A**). When looking at figure 2 A and B, this corresponds to transient plasmid concentrations of 0.015 $\mu g/cm^2$ for Nox1 and NoxA1. Those cells than where transfected with increasing plasmid concentrations of NoxO1. Overexpression of NoxO1 from 0.01 to 0.15 µg plasmid/cm^2 results in an exponential in-

Preprints (www.preprints.org) | NOT PEER-REVIEWED | Posted: 1 March 2023 doi:10.20944/preprints202303.0002.v1

crease of ROS formation (**Figure 5**). Taken into account that transfection efficacy is unaltered by increased plasmid concentrations as seen in figure 4A, the data indicates that a tenfold increase in plasmid concentration per cell roughly triples ROS formation.

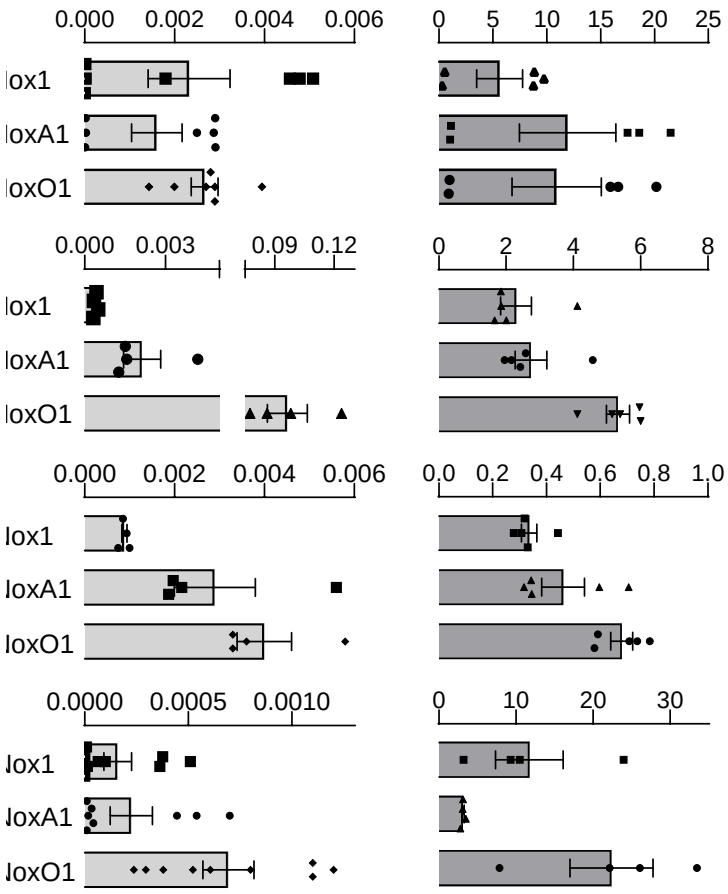

ers of the Nox1 centered

dual cytosolic subunits depicted
5±1) in untreated cells and in
NoxO1. mean±SEM; n=4

Preprints (www.preprints.org) | NOT PEER-REVIEWED | Posted: 1 March 2023 doi:10.20944/preprints202303.0002.v1

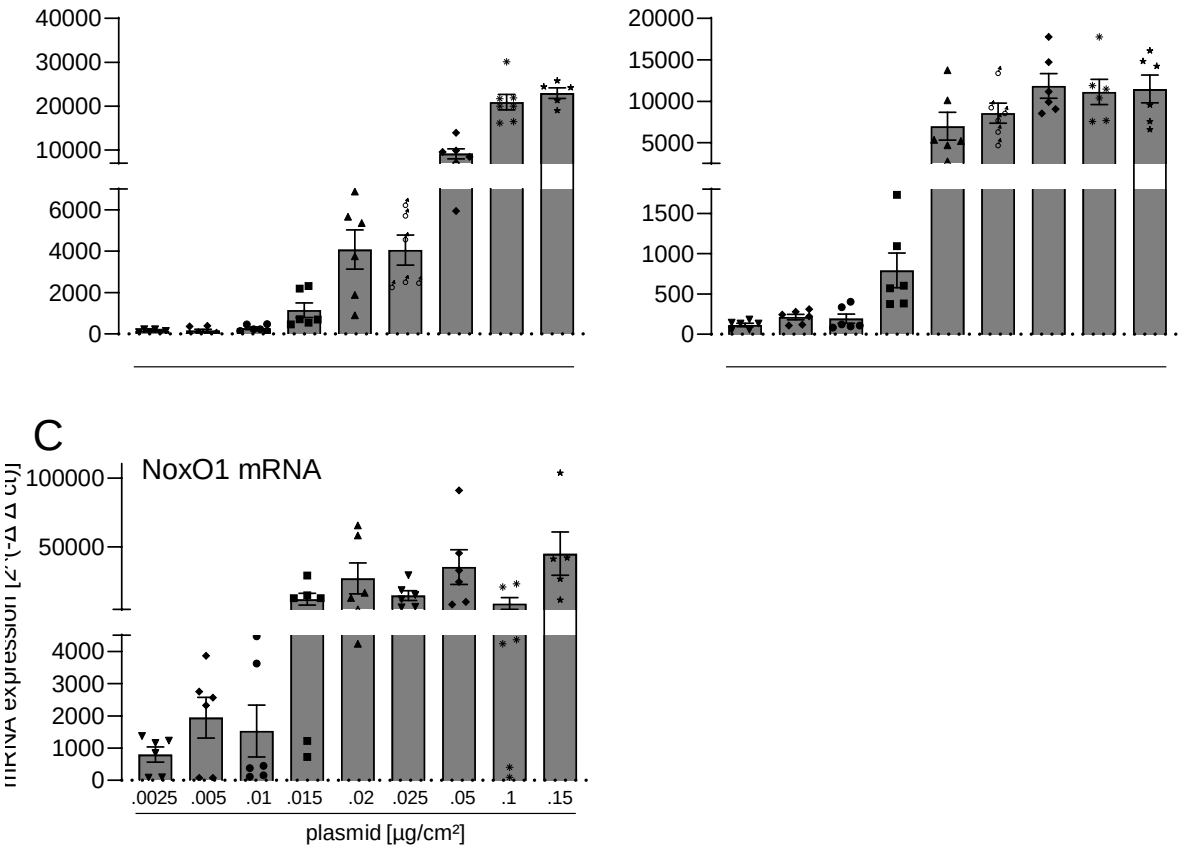

Figure 3: mRNA expression of members of the Nox1 centered NADPH oxidase upon over expression in Hek293 cells.
mRNA expression of Nox1 and of individual cytosolic subunits depicted as relative to mRNA expression in untreated Hek293 cells. mean±SEM; n=3

Preprints (www.preprints.org) | NOT PEER-REVIEWED | Posted: 1 March 2023 doi:10.20944/preprints202303.0002.v1

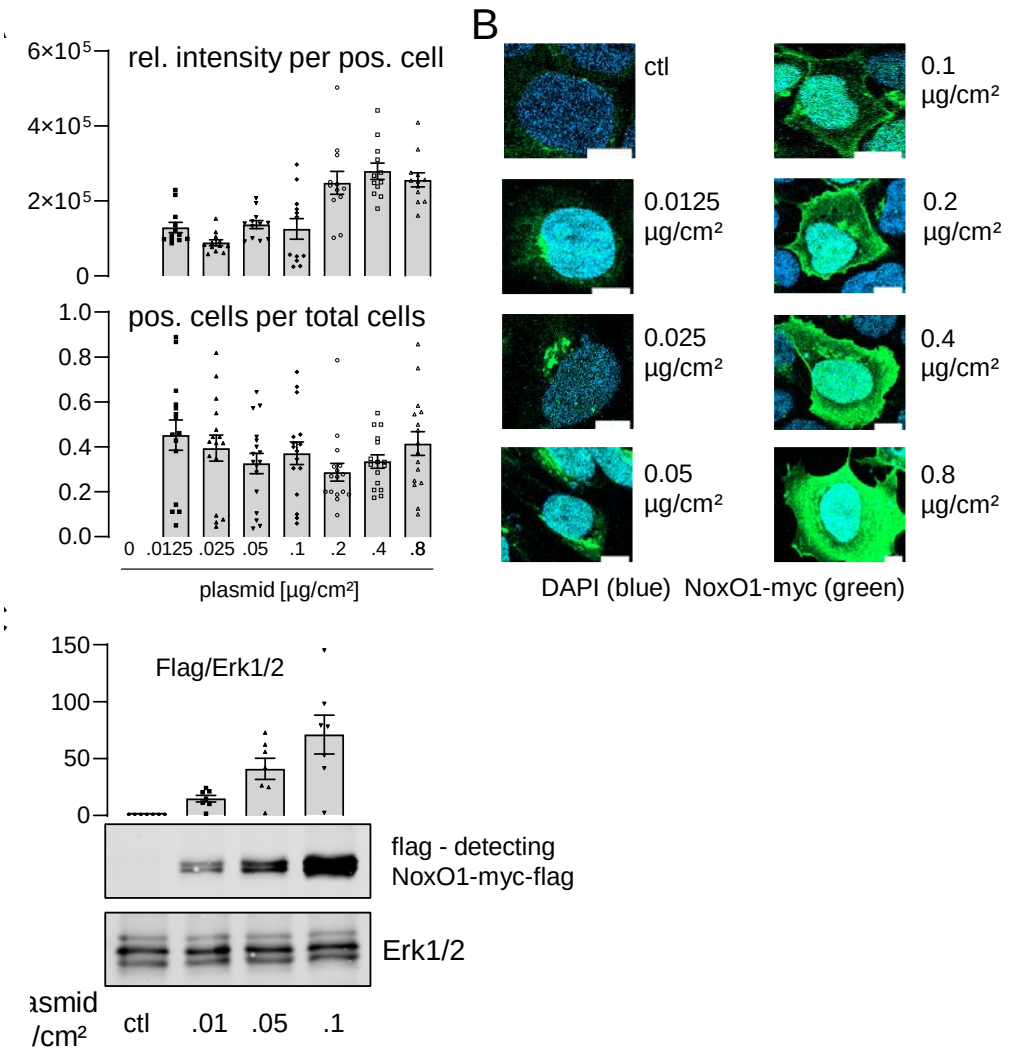

igure 4: NoxO1 cDNA overexpression results in a dose dependent xpression of NoxO1 protein upon over expression in Hek293 cells. oxO1 over expression in Hek293 cells. Statistics (A) of nmunohistochemistry (B) of relative intensity of NoxO1 staining per ɔsitive cell and relative number of transfected cells per well. mean±SEM; =15, scale bar = 10µm

Preprints (www.preprints.org) | NOT PEER-REVIEWED | Posted: 1 March 2023 doi:10.20944/preprints202303.0002.v1

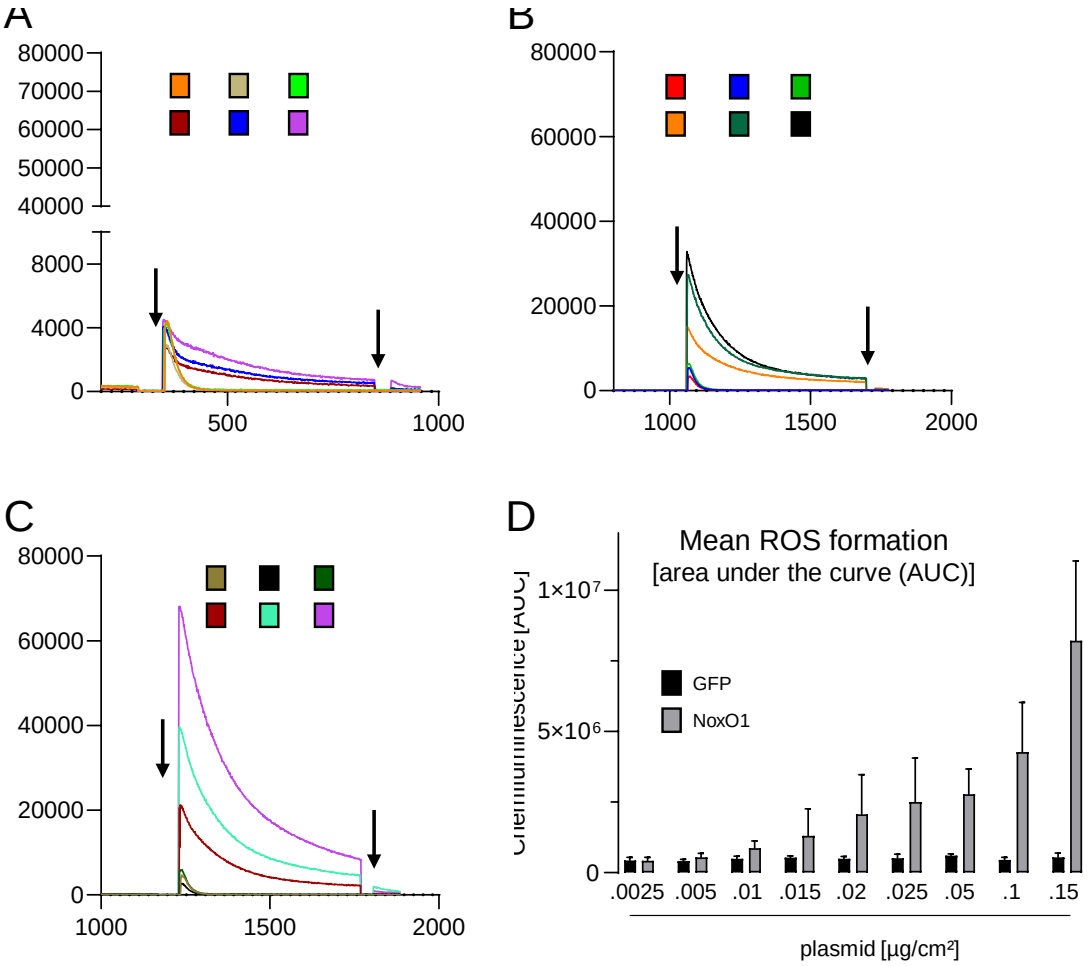

ith constitutive overexpression of Nox1
diated chemiluminescence.
concentration in Hek293-cNox1/NoxA1 cells.

4. Discussion

In the present manuscript, we show that NADPH oxidases are differentially expressed in cancer cells of various origins. However, even though NADPH oxidases were detected in all cells, none of them was producing ROS under basal conditions. This finding contradicts the general assumption of high ROS in cancer cells [15]. Lack of detectable ROS formation may result from culture conditions and may be different in freshly isolated cancer cells or even tissue.

An interesting finding of the present manuscript was that NoxO1 mRNA is more abundant than that of Nox1 and NoxO1. Overexpression of Nox1, NoxA1 and NoxO1 in Hek293 cells did not result in an equal expression of all mRNAs. We can only speculate for the underlying mechanism, which could include more degradation of NoxA1 mRNA compared to Nox1 and NoxO1 as all mRNAs are expressed from the same backbone vector. In native cells and tissue, NoxA1 expression is often expressed at much lower level that NoxO1 or Nox1. Those include retinal ganglion cells [16] Hill et al. found NoxA1 in placenta lower than NoxO1 and both lower than Nox1, which appears to be the main

 doi:10.20944/preprints202303.0002.v1

NADPH oxidase in murine placenta [17]. In fetal brain Nox1, NoxA1 and NoxO1 are equally expressed while fetal liver expresses more NoxA1 than NoxO1 and both more than Nox1 [17]. In murine lung tissue Nox1, NoxA1 and NoxO1 are expressed nearly at the same level, while in colon and heart Nox1 surpluses NoxA1 and NoxO1 [18]. Accordingly, it is obvious that expression of the subunits of the Nox1 centered NADPH oxidase is highly regulated in a tissue specific manner. It may be an interesting object of further studies, how expression of Nox1, NoxA1 and NoxO1 interferes with each other in different cells. Such studies may provide general insights into the regulation of expression of complex subunits.

In case of the Nox1 centered NADPH oxidase, the only known function of the complex subunits is to form the complex and generate ROS. Once assembled, the complex is constitutively active until it departs. Despite the extensive research and identification of several phosphorylation sites in all three components [19], it is not clear, was determines ROS formation by the Nox1 complex. The same holds true for the other constitutive active NADPH oxidase Nox4, which is unique within the family of NADPH oxidases as it directly forms H_2O_2 in a constitutive manner [20]. While Nox4 may be protective by preventing DNA damage and inflammation [21,22], Nox1 promotes DNA damage [23] and knock out of NoxO1 protects female mice from atherosclerosis [24] and longevity in mice [25]. Accordingly, for the treatment of Nox related diseases specific inhibitors are needed, that can prevent ROS formation by one complex without reducing the activity of the other one. A deeper understanding of the molecular mechanisms that activate the Nox1/NoxA1/NoxO1 complex could be beneficial for the search for such inhibitors.

In this study, expression of NoxO1 determines the level of ROS formation by the Nox1 centered NADPH oxidase, even if the level of Nox1 and NoxA1 are unaltered. This is not in line with the assumption of a 1:1:1 ratio of the three components. It rather implies that a surplus of NoxO1 stabilizes the complex and thereby forces ROS formation. It is possible that NoxO1 PRR interacts with SH3 of its siblings. If so, NoxO1 may form a long chain with enhanced binding capacity to the membrane, which could prevent dissociation of the complex. According to this so far unproved model, a perfect inhibitor of Nox1 mediated ROS formation would target NoxO1 at its PX site to prevent translocation to the plasma membrane, its proline rich region to prevent interaction with other NoxO1s and NoxA1 or its SH3 domains to prevent its interaction with p22phox and other NoxO1 [26].

The major finding of this manuscript is that NoxO1 determines the level of ROS formation bey the Nox1 centered NADPH oxidase. Therefore, it is important to note that measuring only Nox1 cannot serve as an indicator for the level of oxidative stress. Rather it is necessary to determine expression level of all subunits, especially NoxO1.

Acknowledgments: This work was supported by the Goethe University Frankfurt am Main, the German Centre for Cardiovascular Research (DZHK) and the DFG excellence cluster Cardiopulmonary Institute (CPI).

Author Contributions: MH: MS and KS designed the experiments. MH, MS and NM performed the experiments. MH and KS analyzed the data. MH and KS wrote the manuscript. All authors interpreted the data and approved the manuscript.

Competing interests statement: The authors have declared that no conflict of interest exists.

References

1. Sumimoto, H.; Minakami, R.; Miyano, K. Soluble Regulatory Proteins for Activation of NOX Family NADPH Oxidases. *Methods Mol. Biol.* **2019**, *1982*, 121–137, doi:10.1007/978-1-4939-9424-3_8.

2. Brandes, R.P.; Weissmann, N.; Schröder, K. Nox family NADPH oxidases: Molecular mechanisms of activation. *Free Radic. Biol. Med.* **2014**, *76*, 208–226, doi:10.1016/j.freeradbiomed.2014.07.046.
3. Schröder, K.; Weissmann, N.; Brandes, R.P. Organizers and activators: Cytosolic Nox proteins impacting on vascular function. *Free Radic. Biol. Med.* **2017**, *109*, 22–32, doi:10.1016/j.freeradbiomed.2017.03.017.
4. Bánfi, B.; Clark, R.A.; Steger, K.; Krause, K.-H. Two novel proteins activate superoxide generation by the NADPH oxidase NOX1. *J. Biol. Chem.* **2003**, *278*, 3510–3513, doi:10.1074/jbc.C200613200.
5. Brandes, R.P.; Harenkamp, S.; Schürmann, C.; Josipovic, I.; Rashid, B.; Rezende, F.; Löwe, O.; Moll, F.; Epah, J.; Eresch, J.; et al. The Cytosolic NADPH Oxidase Subunit NoxO1 Promotes an Endothelial Stalk Cell Phenotype. *Arterioscler. Thromb. Vasc. Biol.* **2016**, *36*, 1558–1565, doi:10.1161/ATVBAHA.116.307132.
6. Xie, Y.; Zhou, X.; Li, J.; Yao, X.-C.; Liu, W.-L.; Xu, P.-S.; Tan, G.-S. Cytotoxic effects of the biflavonoids isolated from Selaginella trichoclada on MCF-7 cells and its potential mechanism. *Bioorg. Med. Chem. Lett.* **2022**, *56*, 128486, doi:10.1016/j.bmcl.2021.128486.
7. Haq, S.; Sarodaya, N.; Karapurkar, J.K.; Suresh, B.; Jo, J.K.; Singh, V.; Bae, Y.S.; Kim, K.-S.; Ramakrishna, S. CYLD destabilizes NoxO1 protein by promoting ubiquitination and regulates prostate cancer progression. *Cancer Lett.* **2022**, *525*, 146–157, doi:10.1016/j.canlet.2021.10.032.
8. Moll, F.; Walter, M.; Rezende, F.; Helfinger, V.; Vasconez, E.; Oliveira, T. de; Greten, F.R.; Olesch, C.; Weigert, A.; Radeke, H.H.; et al. NoxO1 Controls Proliferation of Colon Epithelial Cells. *Front. Immunol.* **2018**, *9*, 973, doi:10.3389/fimmu.2018.00973.
9. Khoshnevisan, R.; Anderson, M.; Babcock, S.; Anderson, S.; Illig, D.; Marquardt, B.; Sherkat, R.; Schröder, K.; Moll, F.; Hollizeck, S.; et al. NOX1 Regulates Collective and Planktonic Cell Migration: Insights From Patients With Pediatric-Onset IBD and NOX1 Deficiency. *Inflamm. Bowel Dis.* **2020**, *26*, 1166–1176, doi:10.1093/ibd/izaa017.
10. Makhezer, N.; Ben Khemis, M.; Liu, D.; Khichane, Y.; Marzaioli, V.; Tlili, A.; Mojallali, M.; Pintard, C.; Letteron, P.; Hurtado-Nedelec, M.; et al. NOX1-derived ROS drive the expression of Lipocalin-2 in colonic epithelial cells in inflammatory conditions. *Mucosal Immunol.* **2019**, *12*, 117–131, doi:10.1038/s41385-018-0086-4.

11. Echizen, K.; Horiuchi, K.; Aoki, Y.; Yamada, Y.; Minamoto, T.; Oshima, H.; Oshima, M. NF-κB-induced NOX1 activation promotes gastric tumorigenesis through the expansion of SOX2-positive epithelial cells. *Oncogene* **2019**, *38*, 4250–4263, doi:10.1038/s41388-019-0702-0.
12. Mirbagheri, S.Z.; Bakhtiari, R.; Fakhre Yaseri, H.; Rahimi Foroushani, A.; Eshraghi, S.S.; Alebouyeh, M. Transcriptional alteration of genes linked to gastritis concerning Helicobacter pylori infection status and its virulence factors. *Mol. Biol. Rep.* **2021**, *48*, 6481–6489, doi:10.1007/s11033-021-06654-w.
13. Proteomics DB. Available online: https://www.proteomicsdb.org/proteomicsdb/#human/proteinDetails/Q8NFA2/expression (accessed on 22 February 2023).
14. GTEx Portal. Available online: https://www.gtexportal.org/home/gene/NOXO1 (accessed on 22 February 2023).
15. Nakamura, H.; Takada, K. Reactive oxygen species in cancer: Current findings and future directions. *Cancer Sci.* **2021**, *112*, 3945–3952, doi:10.1111/cas.15068.
16. Dvoriantchikova, G.; Grant, J.; Santos, A.R.C.; Hernandez, E.; Ivanov, D. Neuronal NAD(P)H oxidases contribute to ROS production and mediate RGC death after ischemia. *Invest. Ophthalmol. Vis. Sci.* **2012**, *53*, 2823–2830, doi:10.1167/iovs.12-9526.
17. Hill, A.J.; Drever, N.; Yin, H.; Tamayo, E.; Saade, G.; Bytautiene, E. The role of NADPH oxidase in a mouse model of fetal alcohol syndrome. *Am. J. Obstet. Gynecol.* **2014**, *210*, 466.e1-5, doi:10.1016/j.ajog.2013.12.019.
18. Mittal, M.; Roth, M.; König, P.; Hofmann, S.; Dony, E.; Goyal, P.; Selbitz, A.-C.; Schermuly, R.T.; Ghofrani, H.A.; Kwapiszewska, G.; et al. Hypoxia-dependent regulation of nonphagocytic NADPH oxidase subunit NOX4 in the pulmonary vasculature. *Circ. Res.* **2007**, *101*, 258–267, doi:10.1161/CIRCRESAHA.107.148015.
19. Brandes, R.P.; Schröder, K. NOXious phosphorylation: Smooth muscle reactive oxygen species production is facilitated by direct activation of the NADPH oxidase Nox1. *Circ. Res.* **2014**, *115*, 898–900, doi:10.1161/CIRCRESAHA.114.305280.
20. Schröder, K. Isoform specific functions of Nox protein-derived reactive oxygen species in the vasculature. *Curr. Opin. Pharmacol.* **2010**, *10*, 122–126, doi:10.1016/j.coph.2010.01.002.

21. Helfinger, V.; Palfi, K.; Weigert, A.; Schröder, K. The NADPH Oxidase Nox4 Controls Macrophage Polarization in an NFκB-Dependent Manner. *Oxid. Med. Cell. Longev.* **2019**, *2019*, 3264858, doi:10.1155/2019/3264858.
22. Helfinger, V.; Freiherr von Gall, F.; Henke, N.; Kunze, M.M.; Schmid, T.; Rezende, F.; Heidler, J.; Wittig, I.; Radeke, H.H.; Marschall, V.; et al. Genetic deletion of Nox4 enhances cancerogen-induced formation of solid tumors. *Proc. Natl. Acad. Sci. U. S. A.* **2021**, *118*, doi:10.1073/pnas.2020152118.
23. Zimnol, A.; Spicker, N.; Balhorn, R.; Schröder, K.; Schupp, N. The NADPH Oxidase Isoform 1 Contributes to Angiotensin II-Mediated DNA Damage in the Kidney. *Antioxidants (Basel)* **2020**, *9*, doi:10.3390/antiox9070586.
24. Buchmann, G.K.; Schürmann, C.; Warwick, T.; Schulz, M.H.; Spaeth, M.; Müller, O.J.; Schröder, K.; Jo, H.; Weissmann, N.; Brandes, R.P. Deletion of NoxO1 limits atherosclerosis development in female mice. *Redox Biol.* **2020**, *37*, 101713, doi:10.1016/j.redox.2020.101713.
25. Schader, T.; Reschke, C.; Spaeth, M.; Wienstroer, S.; Wong, S.; Schröder, K. NoxO1 Knockout Promotes Longevity in Mice. *Antioxidants (Basel)* **2020**, *9*, doi:10.3390/antiox9030226.
26. Schröder, K. NADPH oxidases: Current aspects and tools. *Redox Biol.* **2020**, *34*, 101512, doi:10.1016/j.redox.2020.101512.